Observation of Pheophytin Reduction in Photosystem Two Reaction Centers Using Femtosecond Transient Absorption Spectroscopy†

Gary Hastings,‡ James R. Durrant,‡,§ James Barber,§ George Porter,‡ and David R. Klug*,‡

Photochemistry Research Group, Department of Biology, and AFRC Photosynthesis Research Group, Department of Biochemistry, Imperial College, London SW7 2BB, United Kingdom

Received July 29, 1991; Revised Manuscript Received April 14, 1992

ABSTRACT: Photosystem two reaction centers have been studied using a sensitive femtosecond transient absorption spectrometer. Measurements were performed at 295 K using different excitation wavelengths and excitation intensities which are shown to avoid multiphoton absorption by the reaction centers. Analyses of results collected over a range of time scales and probe wavelengths allowed the resolution of two exponential components in addition to those previously reported [Durrant, J. R., Hastings, G., Hong, Q., Barber, J., Porter, G., & Klug, D. R. (1992) *Chem. Phys. Lett. 188*, 54–60], plus the long-lived radical pair itself. A 21-ps component was observed. The process(es) responsible for this component was (were) found to produce bleaching of a pheophytin ground-state absorption band at 545 nm and the simultaneous appearance of a pheophytin anion absorption band at 460 nm resulting in a transient spectrum which was that of the radical pair $P680^+Ph^-$. This component is assigned to the production of reduced pheophytin. A lower limit of 60% of the final pheophytin reduction was found to occur at this rate. Despite subtle differences in transient spectra, the lifetime and yield of this pheophytin reduction are essentially independent of excitation wavelength within the signal to noise limitations of these experiments. A long-lived species was also observed. This species is produced by those processes which result in the 21-ps component, and it has a spectrum which is found to be independent of excitation wavelength. This spectrum is characteristic of the primary radical pair state $P680^+Ph^-$. In addition, a 200-ps component was found which is tentatively assigned to a slow energy-transfer/trapping process. This component was absent if P680 was excited directly and is therefore not integral to primary radical pair formation. Overall, it is concluded that the rate of pheophytin reduction is limited to $(21\ ps)^{-1}$, even when P680 is directly excited.

The most studied of the isolated photosynthetic reaction centers (RCs)[1] are those from the purple bacteria, particularly *Rhodobacter* (*Rb.*) *sphaeroides* and *Rhodopseudomonas* (*R.*) *viridis*. The electron- and energy-transfer reactions of these complexes have been the subject of intense research dating back to the first isolation of a reaction center from *Rb. sphaeroides* 23 years ago (Reed & Clayton, 1968). Despite the widespread scientific attention that these bacterial RCs have received, and the successful solution of their crystal structures (Deisenhofer et al., 1985; Yeates et al., 1988), the precise mechanism of primary charge separation in these and indeed all RCs remains to be established. Although in global terms purple bacterial RCs contribute less photosynthetic activity than the reaction centers of higher plants, the study of bacterial RCs has arguably produced as much insight to the function of higher plant reaction centers as have more direct lines of research to date.

The photosystem two (PS2) RC of higher plants is of particular interest because it is this reaction center which provides the oxidizing potential for water splitting. The PS2 reaction center was first isolated in 1987, initially by Nanba and Satoh (1987) and then by Barber et al. (1987). This development gave experimental support to the concept that the D1 and D2 polypeptides of PS2 are analogous to the L and M subunits of purple bacteria (Trebst, 1986; Barber, 1987; Michel & Deisenhofer, 1988).

Primary charge separation in PS2 results in the formation of the radical pair state $P680^+Ph^-$. This state is formed in approximately 100 ps in PS2 particles retaining their inner chlorophyll antenna complexes [Nuijs et al., 1986; Schatz et al., 1987; reviewed in Renger (1991)], when P680 is not directly excited. The particles used in these studies contained approximately 80 chlorophylls per reaction center complex, and the rate of radical pair formation was found to be limited by trapping of the excitation energy by the reaction center (Schatz et al., 1988).

The isolation of reaction centers of PS2 has provided an opportunity to study the primary electron-transfer reactions without the complications associated with either energy transfer from large antenna complexes or secondary electron-transfer processes. Excitation of isolated PS2 reaction centers has been shown to result in the formation of the primary radical pair state in less than 25 ps with a near unity quantum yield (Danielius et al., 1987; Booth et al., 1991). The plastoquinones Q_A and Q_B which normally act as the secondary electron acceptors of PS2 are lost during the isolation procedure, preventing secondary electron-transfer reactions. Charge recombination from the primary radical pair state has been found to occur on the nanosecond time scale in the isolated PS2 RC complex (Danielius et al., 1987; Takahashi et al., 1987; Crystall et al., 1989).

The isolated PS2 reaction center was initially thought to be rather difficult to work with due to its inherent instability to light. This instability is to some extent thought to be connected with the physiological phenomenon known as photoinhibition, and the associated degradation and resynthesis

† This work is supported by the AFRC, Royal Society, and SERC. D.R.K. is a Royal Society University Research Fellow.

* Author to whom correspondence should be addressed.

‡ Photochemistry Research Group.

§ AFRC Photosynthesis Research Group.

[1] Abbreviations: RCs, reaction centers; CVL, copper vapor laser; fwhm, full width at half-maximum; PS2, photosystem two; Ph, pheophytin; P680, primary electron donor of PS2.

0006-2960/92/0431-7638$03.00/0

of the D1 polypeptide (Shipton & Barber, 1991; Barber & Andersson, 1991). Although it has been demonstrated that highly active PS2 reaction centers can be isolated (Crystall et al., 1989; Booth et al., 1990), the relative lability of these reaction centers creates a particular problem in ultrafast time-resolved spectroscopic measurements, where exposure to light for long periods is required. It has, however, been demonstrated that, with care, PS2 reaction centers can remain fully active for periods of up to an hour at room temperature and under fairly strong laser illumination (Booth et al., 1990).

Attempts at identifying photochemically generated species from transient absorption spectroscopy (Danielius et al., 1987; Takahashi et al., 1987; Durrant et al., 1990), spectral hole burning (Jankowiak et al., 1989), and deconvolution of absorption spectra (Braun et al., 1990; van Kan et al., 1991) have been made. Previous measurements of radical pair formation in PS2 reaction centers have suggested that the rate of formation of $P680^+Ph^-$ is 3 ps at room temperature (Wasielewski et al., 1989a). Measurements of the thermodynamics associated with radical pair formation (Booth et al., 1990) and identification of multiple radical pair states (Booth et al., 1991) demonstrate that the photochemical detail which can be observed with isolated RCs of PS2 is in some cases similar to that resolved in purple bacterial RCs.

Our most recent assessments of the stoichiometry of a stable and active form of the isolated PS2 reaction centers suggest that the complex contains six chlorophyll molecules, two pheophytins, two β-carotenes, and one cytochrome *b*-559 (Gounaris et al., 1990), which is in agreement with the findings of other workers (Kobayashi et al., 1990). The spectroscopic features of the PS2 RC tend to be more congested and overlapped to a higher degree than in the reaction centers of purple bacteria. This means that particularly sensitive measurements are required to distinguish and identify transient species in time-resolved absorption experiments.

In this paper we demonstrate the application of a highly sensitive femtosecond transient absorption spectrometer to the study of radical pair formation in isolated PS2 reaction centers, using low levels of excitation. We show that the data produced by this apparatus are sufficiently accurate and precise to allow observation and identification of some of the primary electron- and energy-transfer steps which occur in the PS2 reaction center.

We have shown in a previous study (Durrant et al., 1992) that when P680 is directly excited, its singlet excited state decays with lifetimes of 400 ± 100 fs and 3.5 ± 1.5 ps. The primary electron acceptor of PS2 is thought to be a pheophytin molecule (Klimov et al., 1977). The study presented here is an attempt to increase our understanding of the primary photochemistry of PS2 reaction centers by determining the apparent overall rate of pheophytin reduction in this complex. We do not attempt to deduce the route by which the pheophytin is reduced but merely seek to demonstrate that it is possible to time resolve the arrival of an electron at a pheophytin molecule and that the resulting spectrum is that of the radical pair state $P680^+Ph^-$.

MATERIALS AND METHODS

Reaction centers were isolated from pea thylakoid membranes and resuspended in appropriate buffer as in previous measurements (Booth et al., 1991; Chapman et al., 1991). Anaerobic conditions were achieved as previously (Crystall et al., 1989). All transient absorption measurements were performed at 295 K in a 2.5 mm path length cuvette which was rotated at sufficient speed to replace the sample volume between flashes. The optical density of the samples, at the peak of the longest wavelength absorption band (675.5 nm), was between 0.8 and 1.0. Samples were exposed to light from the spectrometer for approximately 1 h, during which time the peak of the long-wavelength absorption band shifted by less than 1 nm, corresponding to less than a 10% loss in activity (Booth et al., 1991). The observed absorption changes were found to be the same, within limits of signal to noise, at the beginning and the end of 1 h of exposure to light in the apparatus.

The femtosecond transient absorption spectrometer is described below. A home-built, colliding-pulse-modelocked dye laser generates pulses with an autocorrelation of 150 fs (fwhm) and energies of 0.16 nJ at 625 nm. These pulses are amplified to 2 μJ using a multipass configuration similar to that described by Knox et al. (1984). The energy for this amplification is provided by the 6.5-kHz, 511-nm beam from a copper vapor laser (CVL) manufactured by Oxford Lasers (U.K.). The amplified pulses are focused into a flowing water cell to generate a femtosecond white light continuum. These white light pulses are split into two parts, one part to form the excitation beam and one part to form the probe beam. The excitation wavelength (612 or 694 nm) is selected from the continuum and reamplified using a second multipass amplifier, pumped by the 578-nm beam from the CVL. After reamplification, the excitation pulses have energies of $\approx$1 μJ, which is reduced to 0.1 μJ before reaching the sample. Group velocity dispersion in both the excitation and probe beams is controlled using two anomalously dispersive delay lines (Fork et al., 1984). The excitation and probe beams are parallel polarized to better than 90%. The excitation beam is focused to a 270-μm waist in the sample (175 μJ cm^{-2}) and the probe beam aligned with the aid of a pinhole to interrogate this excited volume. The main reason for the relatively high sensitivity of these measurements is that signal averaging is performed at 6.5 kHz.

Absorption changes at single wavelengths (detection bandwidth of 2–5 nm) were monitored as a function of time delay using a Michelson interferometer arrangement with a computer-controlled delay line and sensitive difference detection equipment comprising two ratiometers and a lock-in amplifier. The time resolution of the spectrometer was 160 fs, determined by monitoring the 10–90% rise time of absorption changes observed in three dye standards over a wide range of probe wavelengths. The white light probe pulses were temporally dispersed by less than 2 fs/nm between 655 and 700 nm.

Data were collected over two spectral ranges: 420–570 and 655–730 nm. Measurements were made using three time scales, 0–300, 0–80, and 0–13 ps, and two different excitation wavelengths, 612 and 694 nm. Data were collected and analyzed using all permutations of these conditions. Checks were made for consistency between data collected on different time scales. Over 1000 time-resolved decays were analyzed, each consisting of at least 100 data points. The decays were grouped into sets of 12 wavelengths for global analysis. The results of the analysis of the 0–13-ps data have been published elsewhere (Durrant et al., 1992), but all of these data were analyzed together to check for consistency. The time-resolved data at each wavelength are the result of approximately 5 min of signal averaging. Each complete spectrum has been repeated 2–4 times with certain wavelengths repeated up to 12 times. The actual spectra presented are means, and the error bars represent a reproducibility of one standard deviation. Reproducibility of the lifetimes retrieved from the data is also quoted as one standard deviation.

Each decay was analyzed in a number of ways to reduce the effects of exponential correlation and overparametrization (see below).

Lifetimes were calculated by iterative reconvolution based on the Marquardt fitting algorithm assuming multiexponential kinetics according to

$$\Delta OD(\lambda,t) = \sum_i \Delta OD_i(\lambda) \exp(-t/\tau_i) \qquad (1)$$

where $\Delta OD_i(\lambda)$ is the amplitude of a component with a lifetime τ_i at a wavelength λ. The quality of the fits was assessed using a reduced χ^2 criterion and plots of weighted residuals.

Time-resolved decays were analyzed both individually and globally. In the global analyses, up to 12 decays could be analyzed simultaneously with the lifetimes of the components constrained to be the same in all 12 data sets. Global analysis effectively synthesizes higher signal to noise than can be achieved by analyzing a single decay and also reduces the number of free parameters. Global analysis is particularly useful in this study as the spectra of different components are found to dominate the total signal at different wavelengths. In both individual and global analyses one or more of the lifetimes could be fixed, once these had been established from analysis of other data where some components could be more clearly resolved due to the use of a different time scale or spectral range. Pre-exponential factors could be fixed when data sets were individually analyzed. This last option is particularly important as it allows one to assess the effects of long-lived components on the analysis of faster components observed over shorter time scales, where the influence of a long-lived component may not otherwise be easy to ascertain. This method of data analysis makes no allowances for the possible presence of distributions of lifetimes, but such distributions are not required to produce a consistent model for the data presented here.

Estimations of excitation levels, both from the pump beam parameters and independently from the size of the transient bleaches, indicate that only 5–10% of the reaction centers in the volume of the pump beam are excited by each flash.

RESULTS

Absorption difference spectra are presented either as (a) kinetic spectra which represent the difference spectra associated with a particular kinetic component (i.e., spectra of the pre-exponential factors in eq 1), sometimes called decay-associated spectra, or (b) the excitation-induced absorbance difference spectra at a specific time after excitation (all spectra of the nondecaying component can be considered as absorbance difference spectra at long time delays). Positive amplitudes in a kinetic spectrum indicate negative-going absorption changes, and negative amplitudes indicate positive-going absorption changes.

Figure 1 shows spectra of the laser pulses used for excitation compared with the long-wavelength part of the PS2 reaction center absorption spectrum. The spectra of the excitation pulses peak at 612 (10-nm bandwidth) or 694 nm (24-nm bandwidth). The 612-nm pulses are nearly transform limited, but the 694-nm pulses have a much broader spectrum. Transform-limited pulses are not required in experiments of this type unless coherent phenomena are to be investigated. Excitation at 694 nm was used with the intention of exciting P680 directly in a high proportion of reaction centers (see Discussion).

The results described below are also given in Table I.

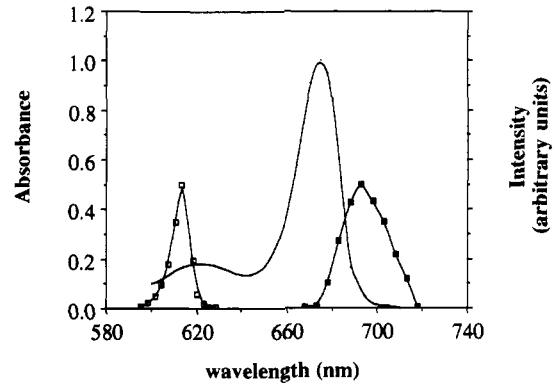

FIGURE 1: Part of the steady-state absorption spectrum of isolated PS2 reaction centers at room temperature (—). Also shown are the spectra of the excitation pulses; these spectra are centered at 612 nm, fwhm 10 nm (□), and 694 nm, fwhm 24 nm (■).

Transient absorption decays between 655 and 700 nm, on a 0–300-ps time scale, with 612-nm excitation, could be well fit by the sum of two exponentials (A2 and A3) and a nondecaying[2] component (A0). Fitting with fewer parameters fails to fit the data. The lifetimes of the exponential components were found to be 18 ± 4 (A2) and 260 ± 70 ps (A3). Of particular note was the finding that the amplitude of the 260-ps component was negligible when 694-nm excitation is used, and in this case the data fit well to a single exponential with a lifetime of 15 ± 5 ps (B2) plus a nondecaying component (B0). This difference between the use of 612- vs 694-nm excitation pulses is illustrated in Figure 2.

Figure 3 shows the kinetic spectra of components A2, A3, and A0 observed following excitation at 612 nm, and Figure 4 shows the spectra of components B2 and B0 following excitation at 694 nm. The spectra of the nondecaying components (A0 and B0) are essentially independent of excitation wavelength and exhibit a pronounced bleaching centered at 681 nm.

The use of a 0–80-ps time scale allows the ~20-ps components (A2 and B2, Figure 2) to be more accurately resolved than on the 0–300-ps time scale. Examples of data collected on the 0–80-ps time scale are shown in Figure 5. Data collected between 655 and 700 nm on the 0–80-ps time scale are well fitted to two exponential components and a nondecaying component, following excitation at either 612 or 694 nm. The lifetimes of the components are 4 ± 2 (A1) and 22 ± 5 ps (A2) following excitation at 612 nm and 4 ± 2 (B1) and 23 ± 5 ps (B2) following excitation at 694 nm. The 260-ps component observed on the 0–300-ps time scale (Figure 2) could not be distinguished from the nondecaying component on the 0–80-ps time scale. Inclusion of the 260-ps component with a fixed lifetime and amplitude during analysis of the 0–80-ps time scale data did not significantly change the lifetime or spectrum of the ~20-ps component (data not shown). This indicates that these two components are well resolved by the fitting procedure. The 4-ps component observed following excitation at either 612 or 694 nm was more clearly resolved on a 0–13-ps time scale. This component, and other fast kinetics, are discussed in detail elsewhere (Durrant et al., 1992).

On a 0–80-ps time scale from 520 to 570 nm, and excitation at either 694 or 612 nm, the data were well fitted to a (19 ± 2)-ps lifetime (A2 and B2) and a nondecaying component

[2] The component defined as "nondecaying" does not decay over the time scales under consideration in this paper. This component actually has a lifetime of tens of nanoseconds.

Table I: Lifetimes Obtained from Global Analyses of Data Presented in This Paper[a]

	lifetime (ps)				
	0–300-ps time scale		0–80-ps time scale		
component	520–570 nm	655–700 nm	445–500 nm	520–570 nm	655–700 nm
612-nm excitation					
A1	NR[b]	NR	–[c]	NR	4 ± 2
A2	23 ± 7	18 ± 4	–	19 ± 2	22 ± 5
A3	~100[f]	260 ± 100	–	NR	NR
A0	nondecaying[d]	nondecaying	–	nondecaying[e]	nondecaying[e]
694-nm excitation					
B1	–	NR	NR	NR	4 ± 2
B2	–	15 ± 5	21 ± 1	19 ± 2	23 ± 5
B0	–	nondecaying	nondecaying	nondecaying	nondecaying

[a] Data were collected on two time scales (0–300 and 0–80 ps), three probe wavelength regions (445–500, 520–570, and 655–700 nm), using either 612- or 694-nm excitation pulses. Data were collected for eight different permutations of these conditions, as indicated in the table, and separate global analyses conducted for each of these permutations. The ~200-ps component observed following excitation at 612 nm (A3) was not observed when 694-nm excitation was used. The 4-ps component is the average of components discussed in more detail elsewhere (Durrant et al., 1991). [b] NR, component not resolved, due to the time scale being inappropriate for the observation of this component and/or the amplitude of this component being too small. [c] –, Data not collected. [d] Nondecaying, a component which did not decay on the time scale of the experiment (see footnote 2). [e] On the 0–80-ps time scale, components A3 and A0 could not distinguished. [f] Amplitude too small to obtain an accurate value for this lifetime.

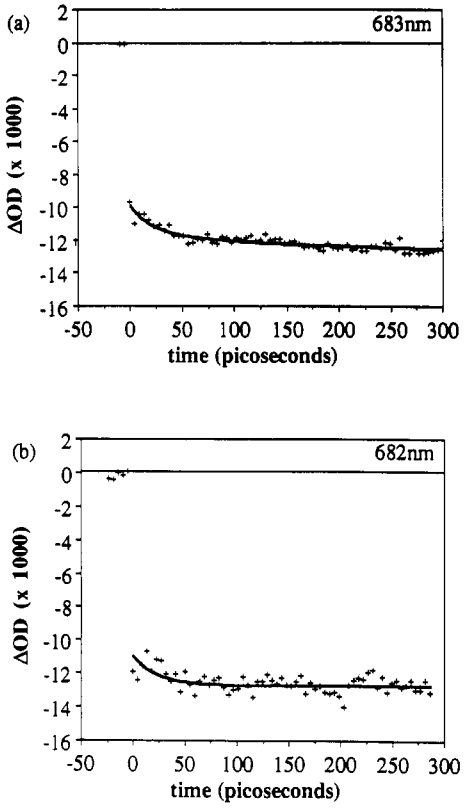

FIGURE 2: Kinetics of the transient absorption change (+) observed between 0 and 300 ps at (a) 683 nm following excitation of PS2 reaction centers at 612 nm and (b) 682 nm following excitation at 694 nm. The solid lines are the fitted functions obtained using eq 1. These are (a) the sum of two exponential components with lifetimes of 18 ± 4 (A2) and 260 ± 70 ps (A3) and a nondecaying component (A0) and (b) the sum of one exponential component with a lifetime of 15 ± 5 ps (B2) and a nondecaying component (B0). Experiments were conducted at 295 K under anaerobic conditions.

(A0 and B0). An example of these data can be seen in Figure 5b. Another component with a lifetime of the order of 100 ps is also present when 612-nm excitation is used (see Figure 6). This component has a small amplitude (which results in a very low precision for the lifetime) and is most easily observed in data collected on the 0–300-ps time scale. Although one cannot be sure that this component is due to the same process which apparently produces a (260 ± 100)-ps lifetime (A3) between 655 and 700 nm, the discrepancy between the lifetimes is within the low precision for these components, and we therefore assume that they represent the same process. There could of course be a genuine wavelength dependence to this component, but our data are not precise enough to determine whether this is in fact the case. Notwithstanding the above, we choose to label the 100-ps component as A3 (see Table I and Figure 6).

Figure 6 shows the kinetic spectra of the (19 ± 2)- and ~100-ps and the nondecaying components in the 520–570-nm spectral region with excitation at (a) 612 and (b) 694 nm. The spectra of the nondecaying components (A0 and B0) exhibit a pronounced bleach centered near 545 nm. Components A2 and B2 both show positive peaks at 545 nm, indicating that these components produce an increased bleaching of the 545-nm band. This is illustrated in Figure 6c, which shows the transient spectra at time delays of 3 and 100 ps. The amplitudes and shapes of the spectra of A0 and B0 in Figure 6 are independent of excitation wavelength to ±20%, as are the amplitudes for A2 and B2.

Data from the 440–500-nm spectral region on a 0–80-ps time scale are well fit by two components when 694-nm excitation is used. One component has a (21 ± 1)-ps lifetime, and the other is nondecaying (see, for example, Figure 5c). The spectra of these components (B2 and B0) are shown in Figure 7.

Essentially identical spectra were recovered for the ~20-ps components (A2 and B2) by analyzing data collected on either the 0–80- or 0–300-ps time scale (data not shown) across all regions of the spectrum. The independent observation of similar lifetimes (20 ps) with the same kinetic spectrum obtained on different time scales, and of similar lifetimes obtained over different spectral ranges (with the exception of A3), is evidence that the fitting procedures are appropriate for these data.

The observed lifetime of the 260-ps component (A3) is likely to be heavily influenced by systematic errors, due largely to the longest time scale used here being somewhat too short to accurately determine the lifetime of this component. It also appears as a (100 ± 100)-ps component between 520 and 570 nm (see above), which merely reflects the low precision for this component due to its small amplitude. Due to the difficulties associated with fitting this component accurately, a more realistic overall value is probably 200 (+300, –100) ps.

We studied the dependence of the transient absorption kinetics upon excitation intensity and determined that identical

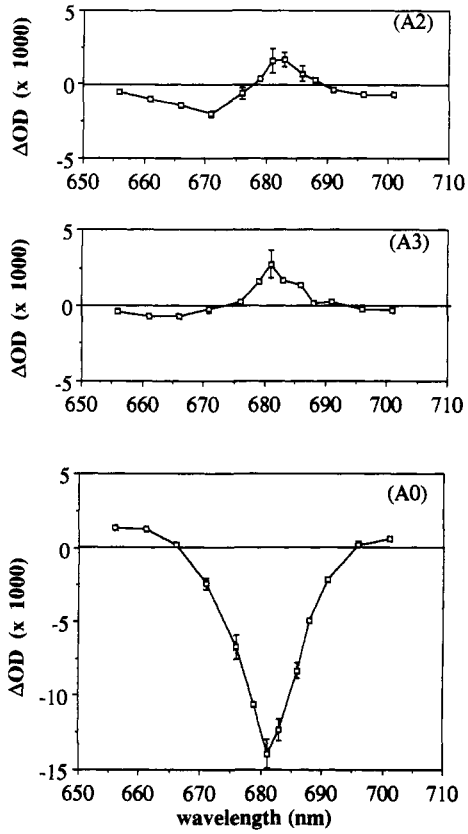

FIGURE 3: Kinetic spectra of components A2 (τ = 21 ps), A3 (τ = 200 ps), and A0 (nondecaying) obtained from single-wavelength transient absorption measurements between 0 and 300 ps and between 0 and 80 ps using 612-nm excitation pulses. Error bars were calculated independently for each data point and where not observable are smaller than the symbols. These kinetic spectra are the spectra of the pre-exponential amplitudes [$\Delta OD_i(\lambda)$] defined in eq 1; therefore, positive amplitudes of these spectra indicate negative-going absorption changes, and negative amplitudes indicate positive-going absorption changes (cf. Figure 2, for example).

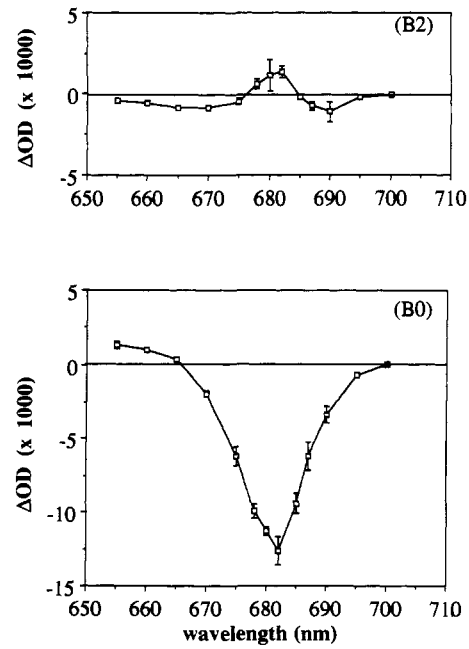

FIGURE 4: Kinetic spectra of components B2 (τ = 21 ps) and B0 (nondecaying) obtained from single-wavelength transient absorption measurements between 0 and 300 ps and between 0 and 80 ps using 694-nm excitation pulses.

kinetics and amplitudes were observed for the 21-ps and non-decaying components for excitation pulses attenuated by up to a factor of 12. This indicates that our estimation that very few reaction centers receive multiple excitations (see Materials and Methods) is indeed correct and that all of the kinetics observed here are due to single photon events.

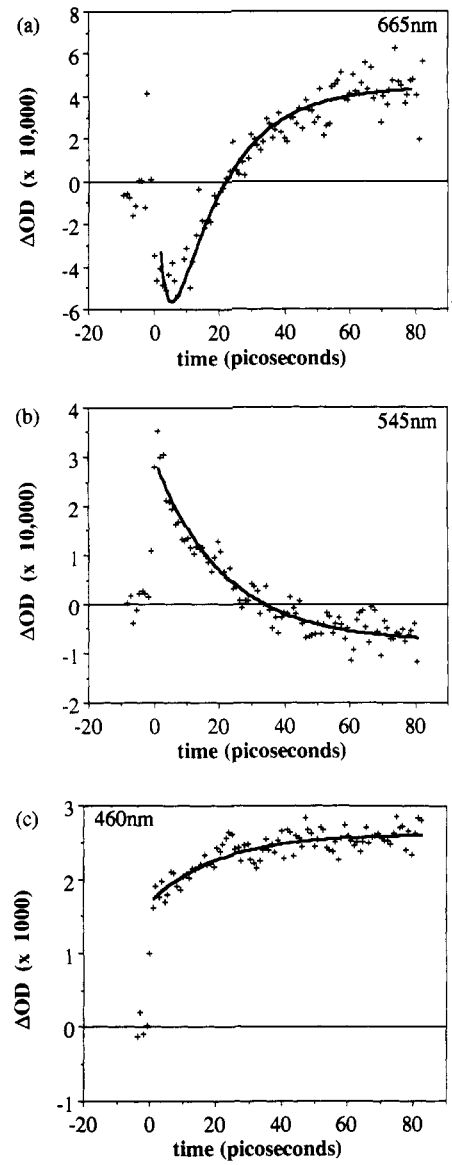

FIGURE 5: Kinetics of the transient absorption changes (+) observed between 0 and 80 ps at (a) 665, (b) 545, and (c) 460 nm following excitation at 694 nm. The solid lines are fitted functions which are the sum of (a) two exponential components with lifetimes of 4 ± 2 (B1) and 23 ± 5 ps (B2) and a nondecaying component (B0) and (b, c) one exponential component with a lifetime of 19 ± 2 (545 nm) or 21 ± 1 ps (460 nm) and a nondecaying component. Component B1 could not be clearly resolved between 440 and 570 nm on the 0–80-ps time scale and was therefore not included in the analysis of data over this spectral range.

DISCUSSION

A summary of data collected on 0–300-, 0–80-, and 0–13-ps time scales is shown in Table II, where data from the 0–13-ps time scale have been taken from Durrant et al. (1992). The final averaged lifetimes of the components discussed in this paper are 200 ± 100 (component A3) and 21 ± 3 ps (for both components A2 and B2) and a nondecaying component (A0 and B0), with the reproducibility quoted as one standard deviation.

The reason for presenting most of the data as kinetic spectra is that most of the kinetic components described above cause

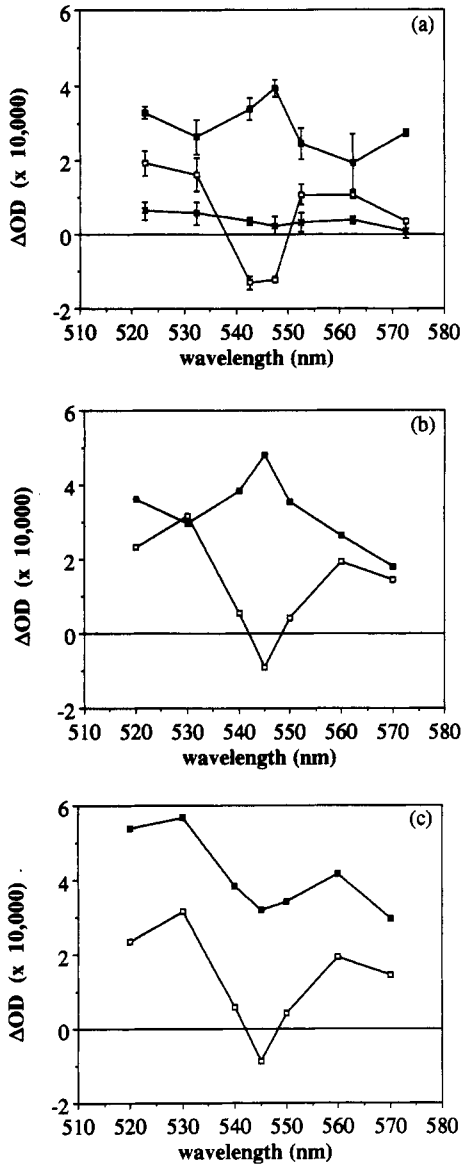

FIGURE 6: Kinetic spectra of 19 ± 2-ps (A2, B2, ■) and nondecaying components (A0, B0, □) obtained from single-wavelength transient absorption measurements between 0 and 300 and between 0 and 80 ps using (a) 612- and (b) 694-nm excitation pulses. Also shown in (a) is the kinetic spectrum of component A3 (×), which is only observed following excitation at 612 nm. (c) Spectra at time delays of 3 (■) and 100 ps (□) following excitation at 694 nm. [The spectra shown in (c) were calculated from the kinetic spectra shown in (b) using eq 1 and are essentially transient absorption spectra before and after the 21-ps component has occurred.]

only relatively small and subtle changes to the overall transient spectra. Although the changes in the overall transient spectrum are small, the high sensitivity of our measurements is quite capable of resolving them. This point is well illustrated by considering Figures 4 and 5a. The largest contribution to the kinetics shown in Figure 5a is that of the 23-ps component (B2), yet Figure 4 demonstrates that the amplitudes of this component are in general much lower than those associated with the nondecaying component (B0).

The results presented above show that optical excitation of isolated PS2 reaction centers results in multiexponential transient absorption kinetics in the picosecond time domain. The use of variable excitation wavelengths is shown to change the relative amplitudes of one of the kinetic components. Excitation pulses of 694 nm were used with the intention of directly exciting P680 in a much higher proportion of reaction centers than is achieved using 612-nm excitation pulses.

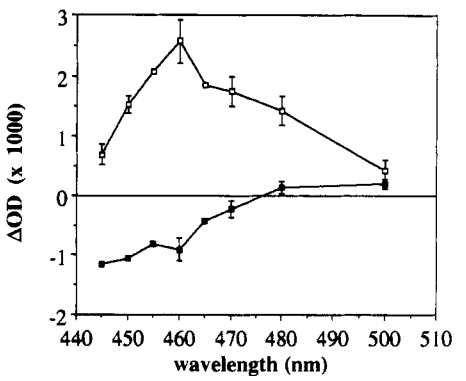

FIGURE 7: Kinetic spectra of 21 ± 1-ps (B2, ■) and a nondecaying component (B0, □) obtained from single-wavelength transient absorption measurements between 0 and 80 ps using 694-nm excitation pulses.

Table II: Summary of the Results of Analysis of Data Presented in This Paper and in Durrant et al. (1991)[a]

(A) 612-nm excitation	(B) 694-nm excitation	assignment
A1,[b] 1.6 ± 0.6 ps	B1,[b] 400 ± 100 fs and 3.5 ± 1.5 ps	loss of P680 singlet excited state
A2, 21 ● 3 ps	B2, 21 ± 3 ps	pheophytin reduction
A3, 200 ± 100 ps	not present	slow energy transfer/trapping
A0, nondecaying	B0, nondecaying	primary radical pair state ($P680^+Ph^-$)

[a] Components B1 and probably A1 are assigned to the decay of a delocalized P680 singlet excited state. They are most clearly resolved on the 0–13-ps time scale and are discussed in detail in Durrant et al. (1991). Components A2 and B2 have similar lifetimes and spectra, although subtle differences in their spectra can be resolved. These components are assigned to pheophytin reduction, which produces the radical pair state $P680^+Ph^-$ (components A0 and B0). Component A3 is only observed following excitation at 612 nm and is assigned to a slow energy-transfer/trapping process. The time scale of $P680^+$ formation is not determined in this paper. The values presented in this table are repeat weighted averages of the data discussed in the text and summarized in Table I. [b] From Durrant et al. (1992).

Complete selectivity is not possible due to the high degree of spectral overlap between individual chromophores in the PS2 reaction center and the finite width of the excitation pulse. As shown in one of our other studies (Durrant et al., 1992), excitation at 694 rather than 612 nm does indeed result in a relatively selective excitation of P680, with this selectivity being retained for at least the first 180 fs.

Radical Pair Spectrum. The nondecaying species observed on the 0–300-ps timescale following excitation at either 612 or 694 nm (Figures 3, 4, 6, and 7) have spectra which support their assignment to the primary radical pair state $P680^+Ph^-$ (Danielius et al., 1987; van Kan et al., 1991; Nuijs et al., 1986; Schatz et al., 1987). Our spectra show a negative feature centered at 681 ± 1 nm assigned largely to the bleaching of P680 and pheophytin Q_y absorption bands, a negative feature centered at 545 ± 2 nm assigned largely to the bleaching of a pheophytin Q_x absorption band, and a positive feature peaking at 460 ± 2 nm assigned largely to the appearance of a pheophytin anion absorption band. The relative amplitudes of these features are 49 (at 681 nm):1 (at 545 nm):6.7 (at 460 nm). The time-resolved radical pair spectrum in the PS2 reaction center has also been measured over this range by Danielius et al. (1987). Their spectrum has a ratio of 51:1:8, which differs from our transient spectrum by less than 20%.

It is also possible to estimate the shape of the radical pair spectrum by combining data from steady-state observations of $P680^+$ and Ph^- in PS2 particles and in vitro (Nanba & Satoh, 1987; Barber et al., 1987; Fujita et al., 1978). Both our data and those of Danielius et al. (1987) are essentially in agreement with what would be predicated from these steady-state observations. For example, the radical pair peaks at 460 nm rather than at 450 nm [which is the peak of the Ph^- band (Nanba & Satoh, 1987)], due to the contribution of $P680^+$ to the difference spectrum (Barber et al., 1987).

The spectra of the nondecaying components are found to be independent of excitation wavelength. This observation is in agreement with previous studies of PS2 RCs which have determined that the primary radical pair state is formed with a near unity quantum yield when a variety of excitation wavelengths are used (Booth et al., 1991). It has also previously been shown that these PS2 samples contain an upper limit of 6% "free" chlorophyll (Booth et al., 1990).

Distinction between the 20- and 200-ps Processes. The similarity in spectra of components A2 (20 ps) and A3 (200 ps) shown in Figure 3 might at first lead one to think that these components might represent the same underlying process. However, the clear distinction between these components from 520 to 570 nm (Figure 6) indicates that the 200-ps component produces very little, if any, of the final nondecaying 545-nm bleach, while the 21-ps component produces ≈60% of the total.

It is important to recognize that the precision of the spectra in Figure 3 (note the small error bars) is sufficiently high that subtle but important differences in shape can be noted. For example, the ratio $A2_{(670nm)}/A3_{(670nm)} = 4$ is distinguishable from $A2_{(680nm)}/A3_{(680nm)} = 0.5$. Consequently, these kinetic spectra clearly do represent different processes as one would expect from a consideration of the data in the 520–570-nm spectral region.

The overall similarity in shape of A2 and A3 between 655 and 700 nm can be rationalized as follows. They both represent processes which bleach the ground state of a relatively low energy (spectroscopically red absorbing) chlorin, accompanied by the ground-state recovery of a slightly higher energy (spectroscopically blue absorbing) chlorin. The mixture of energy/electron-transfer reactions which each of these spectra represent is, however, presumably different, the only connection being that energy is moving overall from high energy (blue) chlorins to lower energy (red) chlorins. Although changes in excited-state absorption do contribute to these spectra, their contribution is likely to be smaller than the prominent features seen in the kinetic spectra of A2, A3, and B2.

The most important distinction between these two processes, however, is that the ≈200-ps component is absent when P680 is excited directly, whereas the ≈20-ps component is present with similar amplitude when either 612- or 694-nm excitation is used.

Slow Energy Transfer/Trapping. The 200-ps component (A3) observed in this study following excitation at 612 nm is most easily assigned to slow energy transfer/trapping within the PS2 RC. The spectrum of the 200-ps component is inconsistent with its assignment to a depolarization process, nor is it likely that this spectrum could result solely from changes in excited-state absorption. The spectrum exhibits a positive feature peaking at 681 nm (Figures 2 and 3). This is due to increased bleaching of a pigment with an absorption maximum near 681 nm and could reflect a degree of slow radical pair formation. This 200-ps component contributes 15 ± 5% of the final absorption change at 681 nm. The negative portion of this component between 655 and 670 nm (Figure 3) is consistent with the ground-state recovery of a chlorin molecule with a Q_y absorption maximum nearer to 670 than to 680 nm. Therefore, the 200-ps component could be assigned to slow energy transfer/trapping from a chlorin with an absorption maximum at a shorter wavelength than P680. This assignment is supported by the observation that the 200-ps component is not observed following excitation at 694 nm.

Earlier measurements on isolated PS2 RCs also observed "slow" energy transfer at 4 K (Wasielewski et al., 1989b), although not at 277 K (Wasielewski et al., 1989a). Our observation of the presence of a slow energy-transfer/trapping process is consistent with recent time-resolved fluorescence studies of PS2 reaction centers (Booth et al., 1991; Roeloffs et al., 1991).

There is the possibility that the 200-ps component could originate from damaged reaction centers in which primary charge separation has been impaired. One might expect to observe this component when exciting at 694 nm as well as 612 nm because the 200-ps component produces a bleach at 680 nm and must therefore originate from reaction centers with pigments which can absorb the 694-nm pulses in the first place. However, as the 200-ps component is not observed using 694-nm excitation, we feel that it is more likely that this component originates from a slow energy-transfer/trapping process rather than a slow electron-transfer reaction, although the latter cannot be definitively ruled out. The spectrum for this component in Figure 6a would suggest that it does not result in the net bleaching of a pheophytin.

The observation of a 200-ps lifetime for an energy-transfer/trapping processing is at first sight surprisingly slow for a complex containing only eight pigments. In bacterial reaction centers the excitation energy is thought to be trapped by the special pair in less than 150 fs (Breton et al., 1986; Johnson et al., 1990). The isolated PS2 RCs used in this study bind two more chlorophylls than reaction centers of purple bacteria (Gounaris et al., 1990). It is possible that the 200-ps component observed here may originate from one or both of these "extra" chlorins being unable to transfer excitation energy rapidly to P680. Energy-transfer rates are strongly dependent upon chromophore separation (proportional to R^{-6}) and orientation. These extra chlorins may be bound to the exterior of the reaction center, thus resulting in the observed slow rate of energy transfer.

In summary, we emphasize that the 200-ps component is not observed when P680 is directly excited; therefore, this component does not seem to be an integral step in primary charge separation by PS2 RCs.

Pheophytin Reduction. At least one of the pheophytin molecules associated with the isolated PS2 RC has a clearly resolved Q_x absorption band with a maximum at 545 nm (Nanba & Satoh, 1987). Bleaching of this band is therefore indicative of the loss of pheophytin ground states. The bleaching of this band is the only spectral feature which can be unambiguously assigned to loss of pheophytin ground states in PS2 RCs, due to the high degree of spectral overlap between chromophores at other wavelengths. Bleaching of the 545-nm band has been observed in previous kinetic studies of PS2 (Danielius et al., 1987; Wasielewski et al., 1989a,b); however, the *rate* of bleaching has not been determined prior to the data which we present here.

The kinetic spectra of the 21-ps components (A2 and B2) exhibit clear maxima at 545 nm (Figure 6) following excitation

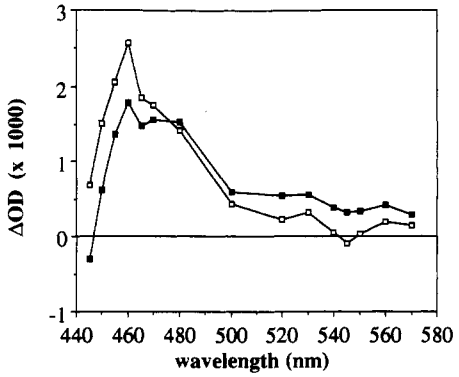

FIGURE 8: Spectra between 445 and 570 nm of optical density changes at time delays of 3 (■) and 100 ps (□) after excitation at 694 nm. (These spectra were calculated from the kinetic spectra shown in Figures 6b and 7 using eq 1 and are essentially transient absorption spectra before and after the 21-ps component has occurred.)

at either 612 or 694 nm and therefore represent a bleaching of this band. The lifetimes of these components are found to be independent of excitation wavelength to ±3 ps.

By comparing the amplitudes of the 21-ps components and the nondecaying (radical pair) components, and taking account of data collected on other time scales, it can be concluded that of the total pheophytin bleached, 60 ± 20% occurs with a rate of 21 ps^{-1} following excitation at 694 nm and 60 ± 20% at the same or similar rate following excitation at 612 nm.

We specifically assign the 21-ps bleaching of the pheophytin Q_x band at 545 nm to pheophytin reduction. This assignment is supported by data obtained between 445 and 570 nm, which is illustrated in Figure 8. This figure shows the absorption difference spectra at 3 and 100 ps after excitation at 694 nm, essentially before and after the 21-ps process (B2) is complete. It is clear from Figure 8 that the 21-ps component results in the appearance of a positive absorption band with a maximum at 460 nm, and the partial recovery of initially positive absorption changes between 480 and 550 nm. Both of these features are consistent with the formation of a pheophytin anion state, and the concomitant decay of chlorophyll excited singlet state(s) (Nanba & Satoh, 1987; Barber et al., 1987; Shepanski & Anderson, 1981). Moreover, the clearest evidence which supports the assignment of the 21-ps components specifically to pheophytin reduction comes from the observation that the nondecaying state produced by the 21-ps component has a spectrum which is, within our signal to noise, that expected for the radical pair state $P680^+Ph^-$ (see Radical Pair Spectrum), whereas the spectrum before the 21-ps component is not that of the radical pair. Combining these observations with the result discussed above (that the 21-ps component results in an increased bleaching of the pheophytin Q_x absorption band), it can be concluded that at least half of the total pheophytin reduction in PS2 RCs occurs at a rate of $(21\ ps)^{-1}$.

The spectra of 21-ps components (A2 and B2) in the 655–690-nm spectral region (Figures 3 and 4) are consistent with previous observations of steady-state pheophytin reduction (Klimov et al., 1977; Nanba & Satoh, 1987) and transient pheophytin anion reoxidation (Nuijs et al., 1986; Schatz et al., 1987) in PS2. However, the 21-ps component (Ph reduction) must result in a change in the redox state of one or more chromophores in addition to pheophytin. This complicates any interpretation of the data because there is a high degree of spectral overlap between chromophores in this spectral region; thus, a complete interpretation of the kinetic spectra of 21-ps components in the Q_y bands is not possible at present.

The two spectra of the 21-ps components between 655 and 670 nm are similar, but subtle differences can be observed when 612- rather than 694-nm excitation is used (spectra A2 and B2 in Figures 3 and 4). These differences could result from the mix of precursor states to the 21-ps component being different when different excitation wavelengths are used. Alternatively, these differences could be a consequence of the two excitation wavelengths exciting reaction centers with different orientational distributions.

The 21-ps components appear to account for only ≈60% of the final pheophytin bleaching (Figure 6). Preliminary analysis of data from the 0–13-ps time scale between 520 and 570 nm indicates that 40% of the pheophytin may be bleached directly by the excitation pulse. Analysis of these data also shows that the processes resulting in the 3.5-ps component (see Table II) produce no increase in the pheophytin Q_x absorption band bleach. This initial bleaching of pheophytin may result from a population of pheophytin excited singlet states formed prior to any electron-transfer processes. In this case, the amplitude of the observed bleaching at 545 nm could underestimate the degree of pheophytin reduction associated with the 21-ps component. In principle, the amplitude of the formation of the pheophytin anion band at 460 nm might allow a more accurate determination of the proportion of pheophytin reduction occurring with a $(21\text{-ps})^{-1}$ rate. Unfortunately, the data in this spectral region (445–500 nm) are not accurate enough to obtain a precise value, particularly as these data will also include contributions from other transient species.

Studies between 655 and 690 nm on the 0–13-ps time scale have shown that 400-fs and 3.5-ps components observed following excitation at 694 nm (Durrant et al., 1992) have spectra which are completely different from that of the 21-ps component. The 400-fs and 3.5-ps components must therefore have different physical origins from that of the 21-ps component observed here. Our results therefore suggest that the 21-ps component observed here could account for all of the pheophytin reduction observed in PS2 RCs following direct excitation of P680.

The amplitude and rate of pheophytin reduction are essentially independent of excitation wavelength (to within ±20% and ±3 ps, respectively), as estimated from data collected between 520 and 570 nm. This indicates that energy/electron-transfer/trapping kinetics result in extensive equilibration of the excitation energy within 21 ps, although the kinetic spectra of the 21-ps components between 655 and 695 nm suggest that these components may proceed from a slightly different mix of precursor states when different excitation wavelengths are used. In addition, as discussed above, there may also be one or two chlorins which are more weakly coupled to the other reaction center pigments. These chlorins are excited only when using the 612-nm pulses, and energy transfer/trapping then occurs with a 200-ps lifetime.

The results presented in this paper do not allow us to determine the rate of oxidation of P680. It has been suggested (Wasielewski et al., 1989a) that the rate of formation of $P680^+Ph^-$ can be determined from the rate of formation of absorption changes at 820 nm. However, as chlorin anion, cation, and excited singlet states all have positive absorption bands of similar magnitudes over this spectral region (Nuijs et al., 1986; Hansson et al., 1988), the observation of kinetics solely at 820 nm may have several possible interpretations. Wasielewski et al. suggest that pheophytin reduction occurs with a 3-ps rate rather than the 21-ps rate which we find (Wasielewski et al., 1989a). Although we do observe a component of ~3 ps (Durrant et al., 1992), it has the opposite

sign to that reported by Wasielewski et al. at 674 nm and must therefore originate from a different process. It is possible that some of these discrepancies arise from their use of a novel isolation procedure (Seibert et al., 1988), but there are also differences in the way in which the experiments were performed. Wasielewski et al. used excitation pulses that were 18 times greater in excitation intensity than those used here (3200 $\mu J/cm^2$ at 610 nm vs 175 $\mu J/cm^2$ at 612 nm), and these produced a maximum bleach 10 times greater than those which we observe. There are also differences between the radical pair spectrum reported by Wasielewski et al. and those reported here and by Danielius et al. (1987). As discussed above, the radical pair spectrum which we report differs from that of Danielius et al. by less than 20%; however, the relative sizes of spectra features from the data of Wasielewski et al. are 24 (682 nm):1 (545 nm):1.4 (460 nm), which differ from our spectrum and that of Danielius et al. by ~200 and 480% for 682 and 460 nm, respectively, when normalized by the amplitude of the dip at 545 nm. There is no obvious way to reconcile the data which we show with those of Wasielewski et al., and we must therefore conclude that the two experiments are observing different processes.

In summary, we have observed an electron transfer in PS2 RCs which results in the production of reduced pheophytin, and this process is found to occur with an overall rate of $(21 \pm 3\ ps)^{-1}$. It is not clear if the observed $(21\text{-ps})^{-1}$ rate essentially corresponds to an underlying electron-transfer rate constant or whether some other processes such as an energy-transfer equilibrium limit the observed rate.

Transient absorption data collected on the 0–13-ps time scale have shown that when P680 is directly excited, some of the P680 singlet excited state decays with lifetimes of 400 fs and 3.5 ps (Durrant et al., 1992). This result does not indicate the rate of $P680^+$ formation or whether pheophytin is reduced directly or as the result of more than one electron-transfer step.

The accumulation of further data is necessary before a complete and testable kinetic model can be developed. In particular, it would be particularly useful if the rate of formation of $P680^+$ formation could be determined. However, our results do show that at least 60% of the pheophytin reduction resulting from primary charge separation in PS2 reaction centers occurs at an effective rate which is approximately 6 times slower than that observed in wild-type reaction centers of *R. viridis* and *Rb. sphaeroides*, despite the extensive homology between these reaction centers and those of photosystem two.

While it is true that one should exercise considerable caution in attempting to connect the observations of this paper to those made in bacterial systems, there does appear to be an intriguing link. The RCs of *Rb. sphaeroides*, *R. viridis*, and *R. capsulatus* all show an approximately $(3.5\text{-ps})^{-1}$ rate of pheophytin reduction at room temperature (Woodbury et al., 1985; Breton et al., 1986; Kirmaier & Holten, 1988). In these RCs the amino acid M208 (M210 for *Rb. sphaeroides*) is a tyrosine; the corresponding amino acid on the L branch (L181) is phenylalanine. These amino acids are of particular interest as they are placed roughly at the central point between the special pair, bacteriopheophytin and bacteriochlorophyll molecules. In one mutant of *Rb. sphaeroides* L181 is preserved as a phenylalanine while M210 is changed to leucine. In these mutated RCs the rate of bacteriopheophytin reduction is lengthened considerably to 22 ± 8 ps (Finkele et al., 1990). The sequences of the D1 and D2 polypeptides line up with sequences of the L and M subunits such that D1-206 corresponds to L181 and D2-206 to M208 (Michel & Deisenhofer, 1988). In pea PS2 RCs D1-206 is a phenylalanine and D2-206 is a leucine, and we show in this paper that the rate of pheophytin reduction appears to be 21 ± 3 ps. It is clear from studies of bacterial mutants (Chan et al., 1991; Nagarajan et al., 1990) that the identity of residues L181 and M208 (M210 in *sphaeroides*) affects the mean rate of pheophytin reduction. The mechanism by which this influence is exercised it not yet understood; nevertheless, the rate of pheophytin reduction in PS2 RCs at room temperature does appear to fit a phenomenological scheme developed for predicting the rate of primary charge separation in bacterial RCs (Chan et al., 1991).

ACKNOWLEDGMENT

We thank Niall Walsh and Caroline Woollin for preparing the reaction center samples and Chris Barnett for excellent technical assistance. We also thank Paula Booth and Linda Giorgi for their helpful comments, Qiang Hong for help with the femtosecond apparatus, Martin Bell for assistance with data analysis, and Oxford Lasers for loan of the copper vapor laser during the early stages of this work. We thank also Graham Fleming for bringing the identity of D2-206 to our attention. We also acknowledge financial support from the Science and Engineering Research Council, the Agriculture and Food Research Council, and the Royal Society.

REFERENCES

Barber, J. (1987) *Trends Biochem. Sci. 12*, 321–326.

Barber, J., & Andersson, B. (1991) *Trends Biochem. Sci. 17*, 61–66.

Barber, J., Chapman, D. J., & Telfer, A. (1987) *FEBS Lett. 220*, 67–73.

Booth, P. J., Crystall, B., Giorgi, L., Barber, J., Klug, D. R., & Porter, G. (1990) *Biochim. Biophys. Acta 1016*, 141–152.

Booth, P. J., Crystall, B., Ahmad, I., Barber, J., Porter, G., & Klug, D. R. (1991) *Biochemistry 30*, 7573–7586.

Braun, P., Greenberg, B. M., & Scherz, A. (1990) *Biochemistry 29*, 10376–10387.

Breton, J., Martin, J.-L., Migus, A., Antonetti, A., & Orszag, A. (1986) *Proc. Natl. Acad. Sci. U.S.A. 83*, 5121–5125.

Chan, C.-K., Chen, L. X-Q., DiMagno, T. J., Hanson, D. K., Nance, S. L., Schiffer, M., Norris, J. R., & Fleming, G. R. (1991) *Chem. Phys. Lett. 176*, 366–372.

Chapman, D. J., Gounaris, K., & Barber, J. (1991) in *Methods in Plant Biochemistry* (Rogers, L., Ed.) pp 171–193, Academic Press, London.

Crystall, B., Booth, P. J., Klug, D. R., Barber, J., & Porter, G. (1989) *FEBS Lett. 249*, 75–78.

Danielius, R. V., Satoh, K., van Kan, P. J. M., Plijter, J. J., Nuijs, A. M., & van Gorkom, H. J. (1987) *FEBS Lett. 213*, 241–244.

Deisenhofer, J., Epp, O., Miki, K., Huber, R., & Michel, H. (1985) *Nature 318*, 618–624.

Durrant, J. R., Giorgi, L. B., Barber, J., Klug, D. R., & Porter, G. (1990) *Biochim. Biophys. Acta 1017*, 167–175.

Durrant, J. R., Hastings, G., Hong, Q., Barber, J., Porter, G., & Klug, D. R. (1992) *Chem. Phys. Lett. 188*, 54–60.

Finkele, U., Lauterwasser, C., Zinth, W., Gray, K. A., & Oesterhelt, D. (1990) *Biochemistry 29*, 8517–8521.

Fork, R. L., Martinez, O. E., & Gordon, J. P. (1984) *Opt. Lett. 9*, 150–153.

Fujita, I., Davis, M. S., & Fajer, J. D. (1978) *J. Am. Chem. Soc. 100*, 6280–6282.

Gounaris, K., Chapman, D. J., Booth, P., Crystall, B., Giorgi, L. B., Klug, D. R., Porter, G., & Barber, J. (1990) *FEBS Lett. 265*, 88–92.

Hansson, O., Duranton, J., & Mathis, P. (1988) *Biochim. Biophys. Acta 932*, 91–96.

Jankowiak, R., Tang, D., Small, G. J., & Seibert, M. (1989) *J. Phys. Chem. 93*, 1649–1654.
Johnson, S. G., Tang, D., Jankowiak, R., Hayes, J. M., Small, G. J., & Tiede, D. M. (1990) *J. Phys. Chem. 94*, 5849–5855.
Kirmaier, C., & Holten, D. (1988) *Isr. J. Chem. 28*, 79.
Klimov, V. V., Klevanik, A. V., Shuvalov, V. A., & Krasnovsky, A. A. (1977) *FEBS Lett. 82*, 183–186.
Knox, W. H., Downer, M. C., Fork, R. L., & Shank, C. V. (1984) *Opt. Lett. 9*, 552–554.
Kobayashi, M., Maeda, H., Watanabe, T., Nakane, H., & Satoh, K. (1990) *FEBS Lett. 260*, 138–140.
Michel, H., & Deisenhofer, J. (1988) *Biochemistry 27*, 1–7.
Nagarajan, V., Parson, W. W., Gaul, D., & Schenk, C. (1990) *Proc. Natl. Acad. Sci. U.S.A. 87*, 7888–7892.
Nanba, O., & Satoh, K. (1987) *Proc. Natl. Acad. Sci. U.S.A. 84*, 109–112.
Nuijs, A. M., van Gorkam, H. J., Plijter, J. J., & Duysens, L. N. M. (1986) *Biochim. Biophys. Acta 848*, 167–175.
Reed, D. W., & Clayton, R. K. (1968) *Biochem. Biophys. Res. Commun. 30*, 471–475.
Renger (1991) *Topics in Photosynthesis Vol. 11, The photosystems: structure, function and molecular biology* (Barber, J., Ed.) Elsevier, Amsterdam, in press.
Roeloffs, T. A., Gilbert, M., Shuvalov, V. A., & Holzwarth, A. R. (1991) *Biochim. Biophys. Acta 1060*, 237–244.
Schatz, G. H., Brock, H., & Holzwarth, A. R. (1987) *Proc. Natl. Acad. Sci. U.S.A. 84*, 8414–8418.
Schatz, G. H., Brock, H., & Holzwarth, A. R. (1988) *Biophys. J. 54*, 397–405.
Seibert, M., Picorel, R., Rubin, A. B., & Connolly, J. S. (1988) *Plant Physiol. 87*, 303–306.
Shipton, C. A., & Barber, J. (1991) *Proc. Natl. Acad. Sci. U.S.A. 88*, 6691–6695.
Takahashi, Y., Hansson, O., Mathis, P., & Satoh, K., (1987) *Biochim. Biophys. Acta 893*, 49–59.
Trebst, A. (1986) *Z. Naturforsch. 41C*, 240–245.
van Kan, P. J. M., Otte, S. C. M., Kleinherenbrink, F. A. M., Nieven, M. C., Aartsma, T. J., & van Gorkom, H. J. (1991) *Biochim. Biophys. Acta 1020*, 146–152.
Wasielewski, M. R., Johnson, D. G., Seibert, M., & Govindjee (1989a) *Proc. Natl. Acad. Sci. U.S.A. 86*, 524–528.
Wasielewski, M. R., Johnson, D. G., Govindjee, Preston, C., & Seibert, M. (1989b) *Photosynth. Res. 22*, 89–99.
Woodbury, N. W., Becker, M., Middendorf, D., & Parson, W. W. (1985) *Biochemistry 24*, 7516–7521.
Yeates, T. O., Komiya, H., Chirano, A., Rees, D. C., Allen, J. P., & Feher, G. (1988) *Proc. Natl. Acad. Sci. U.S.A. 85*, 7993–7997.